Science in China Series E: Technological Sciences

www.scichina.com
tech.scichina.com
www.springerlink.com

Effect of one-step aging on microstructure and properties of a novel Al-Zn-Mg-Cu-Zr alloy

LI XiWu†, XIONG BaiQing, ZHANG YongAn, HUA Cheng, WANG Feng, ZHU BaoHong & LIU HongWei

State Key Laboratory for Fabrication and Processing of Non-ferrous Metals, General Research Institute for Non-ferrous Metals, Beijing 100088, China

The effect of one-step aging temper on the mechanical properties, electrical conductivity and the microstructure of a novel Al-7.5Zn-1.6Mg-1.4Cu-0.12Zr alloy has been investigated. The results indicated that with elevating the aging temperature from 100℃ to 160℃, the aging response rate was greatly accelerated, and the UTS at peak aging condition decreased, while the corresponding TYS increased. However, the electrical conductivity of the alloy became higher. After aging for 24 h at 120℃, the peak UTS and TYS values were achieved as 591 MPa and 541 MPa, respectively; but the alloy achieved a lower conductivity, 20.4 MS/m. When T6 temper was performed at 140℃ for 14 h, the UTS decreased only by 1% of the former, whereas the TYS and the electrical conductivity increased obviously, which were up to 559 MPa and 22.6 MS/m, respectively. The major strengthening precipitates of the peak-aged alloy were GP zones and η' phase. The precipitates in both the matrix and the grain boundary became coarser with rising aging temperature. There were obvious PFZs along the grain boundary both in T6 conditions aged at 140℃ and 160℃.

Al-Zn-Mg-Cu alloy, one-step aging, properties, microstructure

1 Introduction

Al-Zn-Mg-(Cu) (7xxx series) alloys have been widely used in the aerospace industry, due to their desirable specific mechanical properties[1,2]. The Cu-rich 7xxx series alloys include the highest strength of ingot metallurgy Al alloys currently in use in commercial aircrafts: AA7050, AA7150, AA7X49 and AA7055, which generally have a problem to satisfy the need for thicker components due to high quench sensitivity[3]. However, the new generation aircrafts use thicker components than ever because of their large size and today's complex requirements of weight effective performance, durability, damage tolerance, reliability, manufacturability and maintainability. To meet the stringent property requirements at the center of the thick sections, some novel alloys—such as AA7040, AA7140 and AA7085—have been recently developed for this application. Particularly, AA7085 has even lower quench sensitivity and a much higher strength-toughness combination, which has been used for wing spar and rib structures on the new Airbus A380[3−7]. To pursue the alloy development and achieve optimized performance, a novel Al-7.5Zn-1.6Mg-1.4Cu-0.12Zr alloy with modifications in solute content and in particular in Zn/Mg/Cu ratios has been investigated in the present work.

Al-Zn-Mg-Cu alloys are typical aging precipitation strengthening alloys. The usual precipitation sequence of them can be summarized as[8−11]: Solid solution →GP zones $\rightarrow\eta'\rightarrow\eta$ ($MgZn_2$). Metastable η', instead of stable η, is believed to be responsible for peak hardening of these alloys. GP zones and η' phase often form during the early stages of precipitation. The η' phase is a

Received June 16, 2008; accepted Augest 21, 2008
doi: 10.1007/s11431-008-0277-4
†Corresponding author (email: xiwulee@yahoo.com.cn)
Supported by the National Hi-Tech Research and Development Program of China ("863" Project) (Grant No. 2008AA03Z506)

metastable hexagonal phase, semi-coherent with the aluminum matrix. Recently, two types of GP zones, GPI and GPII, have been proposed to form in artificially aged 7xxx series Al alloys. Generally, either GPI or GPII zones can form as precursors of the metastable η' phase[8]. The strong age-strengthening response in 7xxx series alloys is in most cases associated with fine-scale precipitation of the metastable η' phase and its precursors[8,10]. Proper control of the precipitation, especially of the size and density of these precipitates, is therefore crucial in order to obtain optimum microstructure and properties of the alloys. Different aging temperatures have different effects on them. T6 temper can obtain the peak hardness and tensile strength, with high stress corrosion cracking (SCC) susceptivity, which is usually carried out at 120℃[12,13]. In the present work, the effects of one step aging on the properties and microstructure have been investigated in detail.

2 Experimental procedures

The compositions of the experimental alloy was 7.55 wt% Zn, 1.58 wt% Mg, 1.39 wt% Cu, 0.12 wt% Zr, 0.02 wt% Fe, 0.01 wt% Si and balance Al. After casting, the alloy were homogenized and then hot extruded into 25 mm thick plate. Specimens were solution heat treated at 475℃ for 50 min and then water quenched to RT. For the one step aging regimes, the samples were aged at 100℃, 120℃, 140℃ and 160℃ for time up to 88 h, respectively. The mechanical properties and electrical conductivity (MS/m) were measured for selected conditions.

Specimens for TEM were thinned by electropolishing using a twin-jet polisher with a 25% nitric acid solution in methanol at –30℃ and 15—20 V. The specimens were examined in selected area electron diffractioin (SAED) and bright field (BF) imaging modes in a JEOL 2010FX microscope, operating at 200 kV.

3 Results and discussion

3.1 Mechanical properties and electrical conductivity

Figure 1 shows the influence of aging treatment on the mechanical properties and electrical conductivity of the alloy. From Figures 1(a) and (b), it can be found that the ultimate tensile strength (UTS) and tensile yield strength

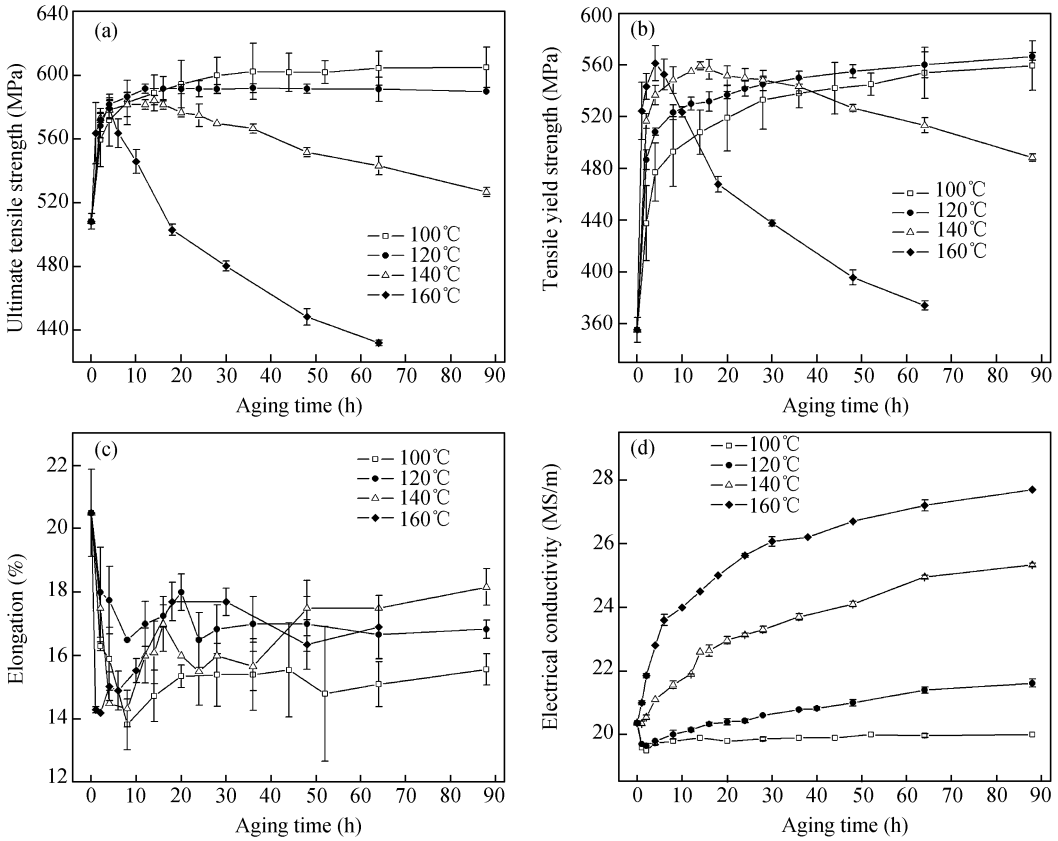

Figure 1 Aging characteristics of the alloy at elevated temperatures: (a) The UTS, (b) TYS, (c) elongation, (d) electrical conductivity.

(TYS) of the alloy increase remarkably before the peak-aged condition is achieved. The UTS and TYS exhibit a faster changed reaction rate at higher aging temperature. The aging time to achieve the peak UTS value is 36 h, 24 h, 14 h and 4 h at 100℃, 120℃, 140℃ and 160℃, respectively. With elevating the aging temperature the peak UTS decreases, while the corresponding TYS increases. After the peak aging stage, the UTS values of the alloy aged at 100℃ and 120℃ keep little change for a relative long time, while the TYS values of them still increase. Figure 1(c) illustrates the ductility decreases rapidly over the time in the early aging period, and recovery of ductility in the overaged condition is not appreciable until severe reduction in strength is encountered. For an optimum compromise for high strength and operating economy, aging at 120℃ for 20—24 h should be used for obtaining T6 properties. As a matter of convenience, the mechanical properties and electrical conductivity of the alloy under T6 temper condition are shown in Table 1.

It is known that the electrical conductivity serves as an indicator of SCC resistance, which has been found to increase with increasing electrical conductivity in Al-Zn-Mg-Cu alloys[14]. From Figure 1(d), it can be seen that the electrical conductivity of the alloy aged at 100℃ remained relatively constant over time; and the electrical conductivity increased rapidly at higher temperatures, indicating that the aging temperature had a dominant role for increasing the conductivity. Loss of coherency and coarsening of precipitates as well as discontinuous and growing grain boundary precipitates will lead to an increase in conductivity. This resulted from the reduction in electron scattering because of the decreasing degree of distortion in the matrix. The increase of the electrical conductivity varied with the aging temperature. By elevating the aging temperature up to 120℃, the electrical conductivity of the alloy appreciably increased. After aging for 24 h at 120℃, the alloy only achieved a lower conductivity, 20.4 MS/m. And the alloy aged at 140℃ for 14 h could achieve a higher conductivity which was up to 22.6 MS/m; furthermore, its UTS only decreased about 7 MPa. Considering the conductivity, T6 temper should be determined as 140℃ for 14 h.

3.2 Microstructure

Figure 2 shows TEM images of precipitates and the SAED patterns of samples in T6 temper. It can be seen that the precipitates in both the matrix and the grain boundary became coarser with rising aging temperature, while the precipitation free zone (PFZ) was present. And most of the precipitates appeared round in the image, and others appeared elongated. After aging for 36 h at 100℃, dark round precipitates with a diameter of 1—2 nm were observed in BF images, as shown in Figures 2(a), (b). Spherical Al_3Zr dispersoids could also be observed (as indicated by the arrow). The grain boundary precipitates were continuous and narrow without the PFZ. With increasing the aging temperature to 120℃, the precipitates grew obviously, their size was about 3—6 nm. The grain boundary precipitates became thick, as shown in Figures 2(d), (e). The precipitates grew quickly at 140℃ and 160℃. After aging for 14 h at 140℃, the size of the precipitates was about 7—10 nm, and the grain boundary precipitates became coarser, semi-continuous and a PFZ of about 10nm width was present, as shown in Figures 2(g), (h). After aging for 4 h at 160℃, the size of the precipitates was even up to 8—15 nm, and the grain boundary precipitates became coarser, semi-continuous and the width of the PFZ increased obviously, which was up to 50 nm approximately.

From the SAED patterns in Al<112> projection of samples, as shown in Figures 2(c), (f), (i) and (l), the presence of sharp diffraction spots at {110} positions could be noted, which were associated with spherical Al_3Zr dispersoids. Diffuse spots near 1/2 {311} associated with the GPII zones were clearly observed; the diffraction features of the η' phases were also clearly observed, such as some diffraction spots and stronger streaks along {111} direction at 1/3 and 2/3 of the {220} positions. Both GPII zones and η' were therefore present

Table 1 Mechanical properties and electrical conductivity of the alloy under T6 temper condition

Aging temper	UTS (MPa)	TYS (MPa)	Elongation (%)	Electrical conductivity (MS/m)
100℃/36 h	602	538	15.4	19.9
120℃/24 h	591	541	16.5	20.4
140℃/14 h	584	559	16.1	22.6
160℃/4 h	580	561	15.0	22.8

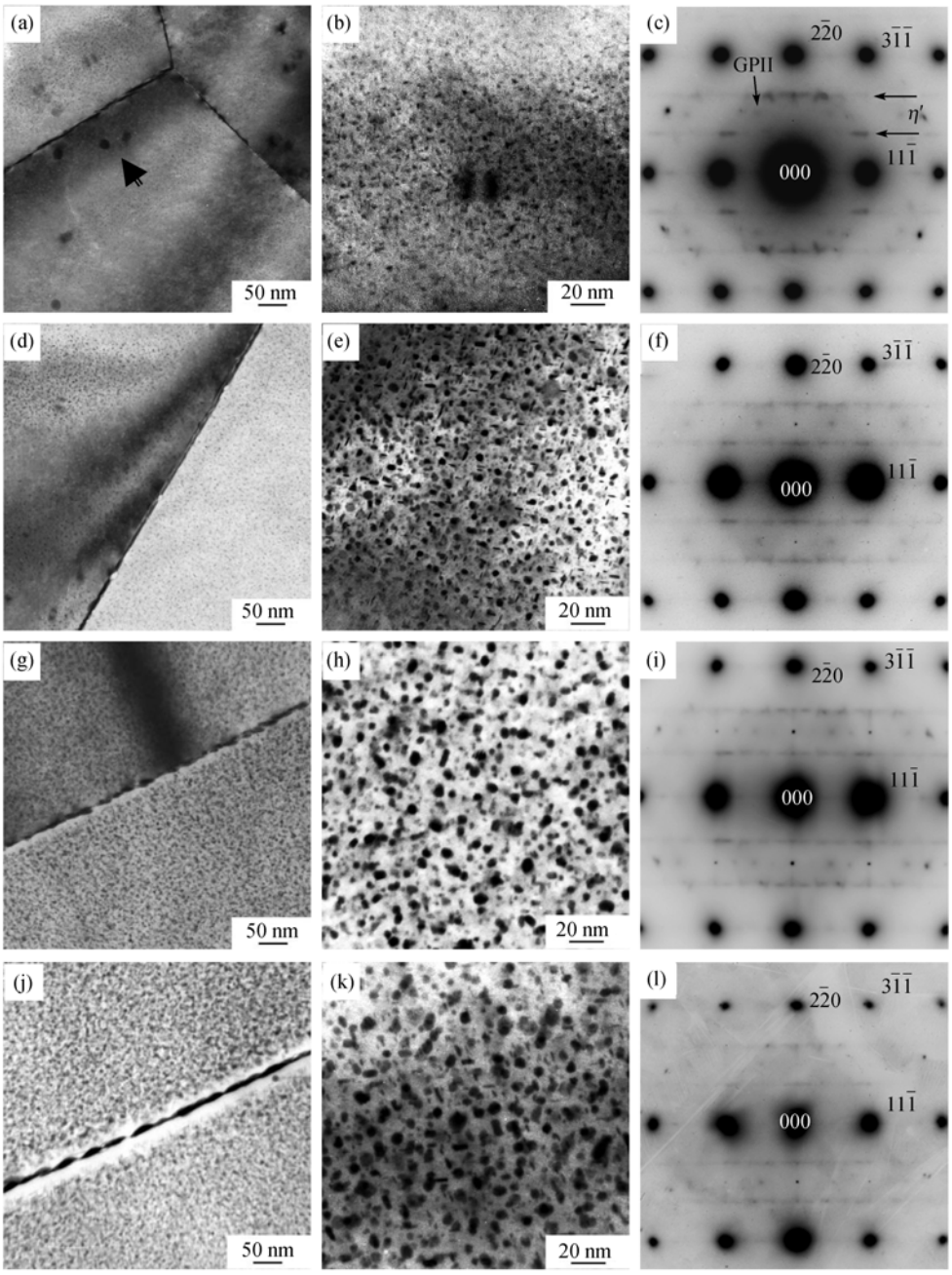

Figure 2 TEM images of precipitates and SAED patterns of samples in T6 temper: (a), (b), (c) 100℃/36 h; (d), (e), (f) 120℃/24 h; (g), (h), (i) 140℃/14 h; (j), (k), (l) 160℃/4 h.

in T6 condition, indicating that the strengthening mechanism of the peak-aged alloy was GP zones and η' phase strengthening in combination. The difference was not significant for the four kinds of T6 treatments mentioned above. After aging for 36 h at 100℃, diffraction spots and streak from η' were weaker as compared with other T6 temper treatment. And after aging for 4 h at 160℃, diffraction spots from GPII zones were weaker as compared with other T6 temper treatment.

Figure 3 shows HREM images taken in the Al-projection [110] of the alloy aged for 24 h at 120℃. Contrast features in the $[110]_{Al}$ projection, as shown in Figure 3(a), were identified as GPII zones, which appeared as thin objects parallel to {111} planes, about 2—3 atom layers thick, 3—7 nm wide. The GPII zones were coherent with the Al matrix, since there was no indication of misfit. And some larger particles about 8 nm wide and approximately 10 atom layers thick were

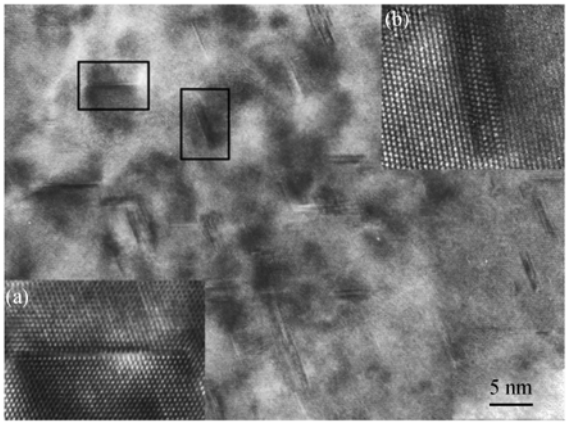

Figure 3 HREM images in [110] projection of the alloy aged for 24 h at 120℃.

found, as shown in Figure 3(b), with some resemblance to the works by Li and Berg[8,9]. According to their theoretical model and experimental results, the η' phase could be identified. This suggested the coexistence of two types of precipitates in the peak-aged alloy, which plays an important role in the age-hardening process.

4 Conclusions

1) The precipitation as well as the mechanical properties and the electrical conductivity were strongly influenced by the aging process. With elevating the aging temperature of 100℃ to 160℃, the aging response rate was greatly accelerated, and the UTS at peak aging condition decreased, while the corresponding TYS increased. However, the electrical conductivity of the alloy became higher.

2) After aging for 24 h at 120℃, the peak UTS and TYS values achieved 591 MPa and 541 MPa, respectively; but the alloy achieved a lower conductivity, 20.4 MS/m. When T6 temper was performed at 140℃ for 14 h, the UTS decreased only by 1% of the former, whereas the TYS and the electrical conductivity increased obviously, which was up to 559 MPa and 22.6 MS/m, respectively.

3) The major strengthening precipitates of the peak-aged alloy are GP zones and η' phase. The precipitates in both the matrix and the grain boundary become coarser with rising aging temperature. There are obvious PFZs along the grain boundary both in T6 conditions aged at 140℃ and 160℃.

The authors are grateful to Professors LIU AnSheng, SHAO BeiLing, and DU ZhiWei for the TEM work.

1 Heinz A, Haszler A, Keidel C, et al. Recent development in aluminium alloys for aerospace applications. Mater Sci Eng A, 2000, 280(3): 102－107
2 John L. Advanced aluminum and hybrid aerostructures for future aircraft. Mater Sci Forum, 2006, 519-521: 1233－1238
3 Warner T. Rencently-developed aluminum solutions for aerospace applications. Mater Sci Forum, 2006, 519-521:1271－1278
4 Chakrabarti D J, Liu J, Sawtell R R, et al. New generation high strength high damage tolerance 7085 thick alloy product with low quench sensitivity. In: Proceedings of ICAA9, Melbourne: Institute of Materials Engineering Australasia Ltd, 2004. 969－974
5 Ilyushenko R, Nesterenkov V. Novel technique for joining of thick section difficult -to-weld aluminium alloys. Mater Sci Forum, 2006, 519-521: 1125－1130
6 Karabin M E, Barlat F, Schultz R W. Numerical and experimental study of the cold expansion process in 7085 plate using a modified split sleeve. J Mater Proc Tech, 2007, 189(1): 45－57
7 Jabra J, Romios M, Lai J, et al. The effect of thermal exposure on the mechanical properties of 2099-T6 die forgings, 2099-T83 extrusions, 7075-T7651 plate, 7085 -T7452 die forgings, 7085-T7651 plate, and 2397-T87 plate aluminum alloys. J Mater Eng Perform, 2006, 15(5): 601－607
8 Li X Z, Hansen V, Gjφnnes J, et al. HREM study and structure modeling of the η' phase, the hardening precipitates in commercial Al–Zn–Mg alloys. Acta Mater, 1999, 47(9): 2651－2659
9 Berg L K, Gjφnnes J, Hansen V, et al. GP-zones in Al–Zn–Mg alloys and their role in artificial aging. Acta Mater, 2001, 49(12): 3443－3451
10 Jiang X J, Noble B, Holme B, et al. Differential scanning calorimetry and electron diffraction investigation on low-temperature aging in Al-Zn-Mg alloys. Metall Mater Trans A, 2000, 31(2): 339－348
11 Gjφnnes J, Simensen Chr J. An electron microscope investigation of the microstructure in an aluminium-zinc-magnesium alloy. Acta Metall, 1970, 18: 881－890
12 Gang S, Alfred C. Early-stage precipitation in Al-Zn-Mg-Cu alloy (7050). Acta Mater, 2004, 52(15): 4503－4516
13 Fan X G, Jiang D M, Meng Q C, et al. Characterization of precipitation microstructure and properties of 7150 aluminium alloy. Mater Sci Eng A, 2006, 427(1): 130－135
14 Starink M J, Li X M. A model for the electrical conductivity of peak-aged and overaged Al-Zn-Mg-Cu alloys. Metall Mater Trans A, 2003, 34A(4): 899－911